

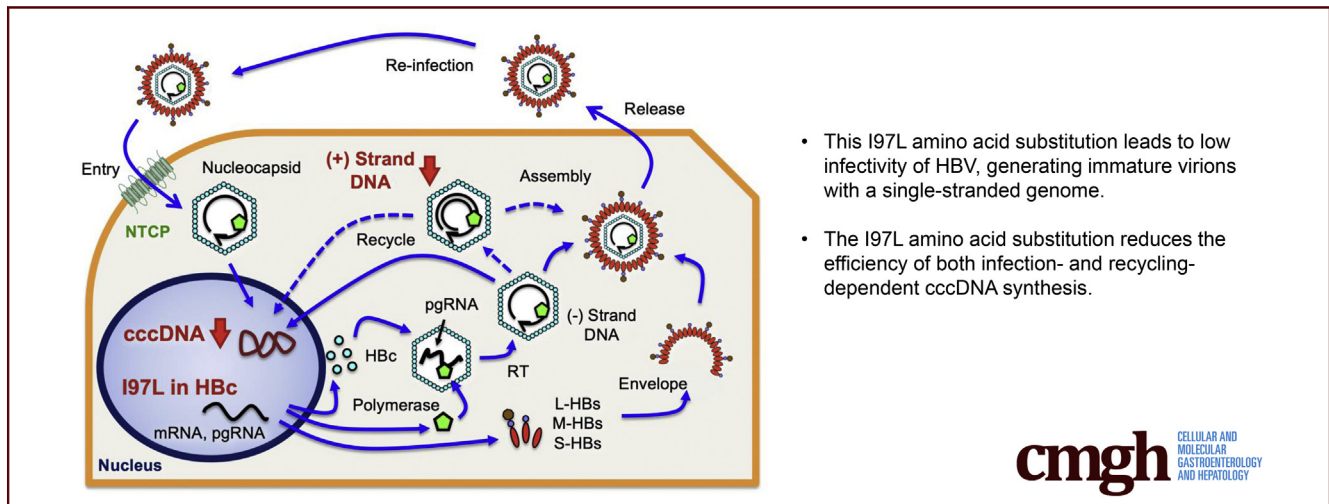
ORIGINAL RESEARCH

Amino Acid Polymorphism in Hepatitis B Virus Associated With Functional Cure



Takashi Honda,¹ Norie Yamada,² Asako Murayama,² Masaaki Shiina,² Hussein Hassan Aly,² Asuka Kato,¹ Takanori Ito,¹ Yoji Ishizu,¹ Teiji Kuzuya,¹ Masatoshi Ishigami,¹ Yoshiki Murakami,³ Tomohisa Tanaka,⁴ Kohji Moriishi,⁴ Hironori Nishitsuji,⁵ Kunitada Shimotohno,⁵ Tetsuya Ishikawa,¹ Mitsuhiro Fujishiro,¹ Masamichi Muramatsu,² Takaji Wakita,² and Takanobu Kato²

¹Department of Gastroenterology and Hepatology, Nagoya University Graduate School of Medicine, Nagoya; ²Department of Virology II, National Institute of Infectious Diseases, Tokyo; ³Department of Molecular Pathology, Tokyo Medical University, Tokyo; ⁴Department of Microbiology, Graduate School of Medicine, University of Yamanashi, Yamanashi; and ⁵Genome Medical Sciences Project, National Center for Global Health and Medicine, Ichikawa, Japan



cmgh CELLULAR AND MOLECULAR GASTROENTEROLOGY AND HEPATOLOGY

SUMMARY

The amino acid substitution I97L in the HBC region is associated with stable hepatitis achieving a functional cure with the sustained loss of HBsAg. This substitution leads to low level of cccDNA via the production of an immature virion with a single-stranded genome.

BACKGROUND & AIMS: To provide an adequate treatment strategy for chronic hepatitis B, it is essential to know which patients are expected to have a good prognosis and which patients do not require therapeutic intervention. Previously, we identified the substitution of isoleucine to leucine at amino acid 97 (I97L) in the hepatitis B core region as a key predictor among patients with stable hepatitis. In this study, we attempted to identify the point at which I97L affects the hepatitis B virus (HBV) life cycle and to elucidate the underlying mechanisms governing the stabilization of hepatitis.

METHODS: To confirm the clinical features of I97L, we used a cohort of hepatitis B e antigen–negative patients with chronic hepatitis B infected with HBV-I97L wild-type (wt) or HBV-I97L. The effects of I97L on viral characteristics were evaluated by in vitro HBV production and infection systems with the HBV reporter virus and cell culture-generated HBV.

RESULTS: The ratios of reduction in hepatitis B surface antigen and HBV DNA were higher in patients with HBV-I97L than in those with HBV-I97wt. HBV-I97L exhibited lower infectivity than HBV-I97wt in both infection systems with reporter HBV and cell culture-generated HBV. HBV-I97L virions exhibiting low infectivity primarily contained a single-stranded HBV genome. The lower efficiency of cccDNA synthesis was demonstrated after infection of HBV-I97L or transfection of the molecular clone of HBV-I97L.

CONCLUSIONS: The I97L substitution reduces the level of cccDNA through the generation of immature virions with single-stranded genomes. This I97L-associated low efficiency of

cccDNA synthesis may be involved in the stabilization of hepatitis. (*Cell Mol Gastroenterol Hepatol* 2021;12:1583–1598; <https://doi.org/10.1016/j.jcmgh.2021.07.013>)

Keywords: HBc; cccDNA; HBVcc.

More than 250 million people worldwide are infected with hepatitis B virus (HBV). HBV infection is responsible for two-thirds of hepatitis cases worldwide, and the number of HBV-related deaths is high and increasing among patients with serious infectious diseases such as tuberculosis, human immunodeficiency virus, and malaria.¹ Although several trials have been conducted to eliminate HBV from infected patients, the strategy for a complete cure has not yet been established because the eradication of covalently closed circular DNA (cccDNA) in the nucleus of infected hepatocytes cannot be achieved by the current treatment strategies.^{2,3} Therefore, to develop new therapeutics, it is important to understand the pathophysiology of chronic hepatitis B (CHB) and the virologic characteristics of HBV. CHB is a progressive disease that develops into cirrhosis and hepatocellular carcinoma. However, in limited cases, it becomes stable hepatitis characterized by a low level of HBV DNA and normal alanine aminotransferase (ALT). Such a status can be achieved through the sustained loss of hepatitis B surface antigen (HBsAg), defined as a functional cure, and patients who achieve a functional cure are considered to have a good prognosis, which is a current goal of treatment for CHB.^{4–7} On the other hand, for patients with active hepatitis, therapeutic intervention such as interferon (IFN)-based and/or nucleos(t)ide analog (NA) therapy is required to reduce HBV DNA and ALT levels.^{8–10} However, IFN-based therapy is associated with considerable side effects, and NA therapy has some problems with the emergence of resistant strains and deterioration of renal function, and it also requires long-term use.^{11,12} To provide an adequate treatment strategy, it is essential to predict patients with a good prognosis who do not require therapeutic intervention.


Previously, we analyzed patients infected with HBV genotype C and compared the full-genome sequences of HBV between patients with active and stable hepatitis. We identified the characteristic substitution of isoleucine with leucine at amino acid 97 (I97L) in the hepatitis B core (HBc) region among those with stable disease.¹³ HBV-I97L was mainly detected in hepatitis B e antigen (HBeAg)-negative patients, and the patients infected with HBV-I97L exhibited low levels of HBsAg and HBV DNA and achieved ALT within the normal range. In this study, we aimed to confirm the involvement of the I97L substitution in the observed ALT within the normal range and reductions in HBV DNA and HBsAg among HBeAg-negative patients. We also analyzed the effects of this substitution on the HBV life cycle to clarify the underlying mechanisms for the stabilization of hepatitis by using HBV production and infection models with cell culture.

Results

Clinical Characteristics and Transition of HBV DNA and HBsAg Levels in Patients Infected With HBV-I97wt or HBV-I97L

HBeAg-negative patients (n = 77; [Figure 1](#)) were divided into 2 groups according to the amino acid, isoleucine (HBV-I97wt) or leucine (HBV-I97L), at position 97 in the HBc region. Thirty-seven patients were included in the HBV-I97wt-infected group, and 40 patients were included in the HBV-I97L-infected group ([Table 1](#)). We found the 4 patients infected with the mixed I97 species in analysis by the direct sequencing. These patients were included in each group according to the major I97 species. Between these groups, the sex ratio and mean age were matched; at the start of the observation, there was no significant difference in the levels of ALT, HBsAg, HBV DNA, or other clinical parameters related to liver function. At the end of the observation, the number of patients who achieved ALT within the normal range was higher in the HBV-I97L-infected group than in the HBV-I97wt-infected group. Levels of HBsAg and HBV DNA were significantly lower in patients with HBV-I97L than in those with HBV-I97wt ($P = .029$ and $<.0001$, respectively). The mean observation periods of these groups were comparable. We also compared the transitions of HBsAg and HBV DNA ([Table 2](#), [Figure 2](#)). Among patients with HBV-I97wt, HBsAg and HBV DNA became undetectable in only 3 (8.1%) and 4 (10.8%) patients, respectively. In contrast, HBsAg and HBV DNA became undetectable in 11 (27.5%) and 14 (35.0%) patients with HBV-I97L, respectively. These rates of undetectable HBsAg and HBV DNA levels were significantly higher in patients with HBV-I97L than in those with HBV-I97wt ($P = .028$ and $.012$, respectively). We also compared the annual reduction in HBV DNA and HBsAg levels between these groups. The annual reduction in HBsAg in patients with HBV-I97L was -0.25 ± 0.28 log IU/mL and was significantly greater than that in those with HBV-I97wt (-0.12 ± 0.22 log IU/mL; $P = .029$). The annual reduction in HBV DNA in the patients with HBV-I97L was -0.36 ± 0.53 log copies/mL and was also significantly greater than that in those with HBV-I97wt (-0.12 ± 0.44 log copies/mL; $P = .030$). The patients infected with mixed I97 species exhibited similar clinical features with other patients in the same groups (data not shown).

Abbreviations used in this paper: ALT, alanine aminotransferase; cccDNA, covalently closed circular DNA; CHB, chronic hepatitis B; DAPI, 4',6-diamidino-2-phenylindole; GEq, genome equivalent; HBc, hepatitis B core; HBcrAg, hepatitis B core-related antigen; HBeAg, hepatitis B e antigen; HBsAg, hepatitis B surface antigen; HBV, hepatitis B virus; HBVcc, cell culture-generated HBV; IFN, interferon; NA, nucleos(t)ide analog; NL, NanoLuc luciferase; PCR, polymerase chain reaction; pgRNA, pregenomic RNA; RC, relaxed-circular HBV DNA; RLU, relative light units; RT, reverse transcription; SD, standard deviation; SDS, sodium dodecyl sulfate; SS, single-stranded HBV DNA; wt, wild-type.

 Most current article

© 2021 The Authors. Published by Elsevier Inc. on behalf of the AGA Institute. This is an open access article under the CC BY-NC-ND license (<http://creativecommons.org/licenses/by-nc-nd/4.0/>).

2352-345X

<https://doi.org/10.1016/j.jcmgh.2021.07.013>

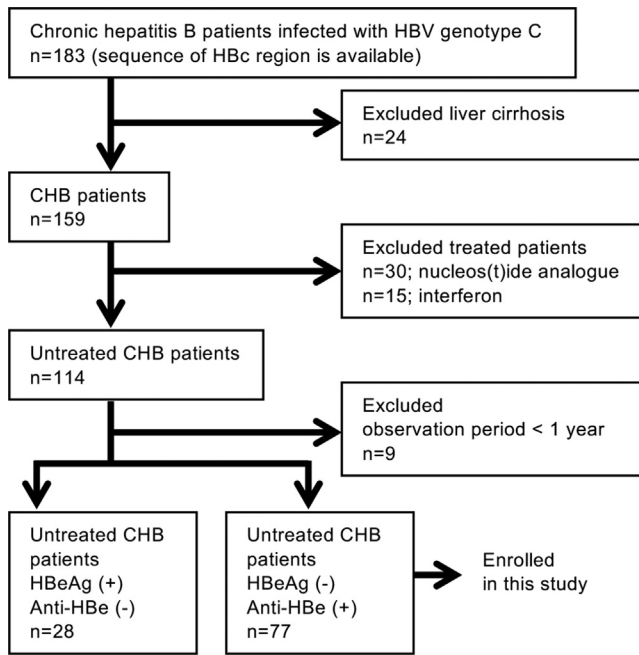


Figure 1. Inclusion and exclusion criteria of patients enrolled in this study. Serum samples were collected from 183 CHB patients infected with HBV genotype C to obtain written informed consent. Twenty-four patients were excluded because of liver cirrhosis. Thirty patients were also excluded because of treatment with NAs, and 15 patients were excluded because of treatment with IFN. Nine patients were excluded because their follow-up period was <1 year. Of the remaining 105 patients, 77 patients were HBeAg negative and enrolled.

Effects of I97L in the HBV Reporter Virus Infection System

To assess the effects of amino acid substitution I97L in the HBc region on the HBV life cycle, we used an infection system with recombinant HBV reporter virus (HBV/NL) encoding NanoLuc luciferase (NL).¹⁴ We prepared 2 kinds of encapsidation signal-lacking plasmids (HBV-dE) containing

I97wt and I97L and transfected them with the encapsidation competent-reporter plasmid (HBV-NL) into HepG2 cells to obtain the HBV reporter viruses I97wt-HBV/NL and I97L-HBV/NL (Figure 3A).¹⁵ HBsAg levels in the culture medium were comparable between I97wt-HBV/NL and I97L-HBV/NL. The culture medium level of hepatitis B core-related antigen (HBcrAg) was higher for I97wt-HBV/NL, whereas the NL DNA titer was lower in I97L-HBV/NL than in I97wt-HBV/NL (Figure 3B). When infected with I97wt-HBV/NL and I97L-HBV/NL at 20 genome equivalents (GEq) per cell, NL activity was substantially (approximately 4-fold) lower in I97L-HBV/NL-infected cells than in I97wt-HBV/NL-infected cells (Figure 3C).

To compare the efficiencies of infectious virus production associated with enveloping, we analyzed the generated HBV/NLs by iodixanol density gradient, applying the same amount of HBsAg. For the density gradient of I97wt-HBV/NL, HBsAg peaked at fraction 13, and HBcrAg peaked at fraction 16. NL DNA showed 2 peaks at fractions of 13 and 17 (Figure 3D, upper panels). A similar profile was observed for the density gradient of I97L-HBV/NL, a peak of HBsAg at fraction 13 and 2 peaks of NL DNA at fractions of 13 and 17 (Figure 3E, upper panels). In this density gradient, HBcrAg had 2 peaks at fractions 13 and 16. These peaks were considered to contain enveloped (fraction 13) or naked capsids (fraction 16).¹⁶ In the case of I97L-HBV/NL, the amount of HBcrAg in fraction 16 decreased, with another peak at fraction 13. These data suggested that the amount of HBc protein that interacts with HBsAg increased for I97L-HBV/NL. The NL DNA level in the peak fraction was lower for I97L-HBV/NL than for I97wt-HBV/NL, depending on the difference in NL DNA titer in the culture media. Infection with the same amount from the fractions of these gradients revealed lower infectivity for I97L-HBV/NL than for I97wt-HBV/NL (Figure 3D and E, lower panels). At the peak fraction of infectivity, the mean infectivity titer adjusted by NL DNA was 165.0 ± 3.3 and 49.9 ± 5.4 (relative light units [RLU]/copy) for I97wt- and I97L-HBV/NL, respectively (Table 3).

Table 1. Clinical Characteristics of Patients With I97wt or I97L at Baseline

	Total (n = 77)	HBV-I97wt (n = 37)	HBV-I97L (n = 40)	P value ^a
Sex (male/female)	35/42	18/19	17/23	.588
Age (y)	45.2 ± 11.5	47.6 ± 11.8	42.9 ± 10.9	.076
ALT (IU/L)	39.0 ± 43.3	33.8 ± 28.2	43.8 ± 53.7	.303
ALT within the normal range (<30 IU/L)	49 (63.6%)	22 (59.5%)	27 (67.5%)	.464
Gamma-glutamyl transpeptidase (IU/L)	27.1 ± 21.1	29.0 ± 23.3	25.3 ± 18.8	.451
Total bilirubin (mg/dL)	0.8 ± 0.3	0.9 ± 0.4	0.8 ± 0.3	.203
Albumin (g/dL)	4.3 ± 0.5	4.4 ± 0.7	4.2 ± 0.4	.207
Platelet count ($\times 10^4/\mu\text{L}$)	19.4 ± 5.5	19.2 ± 7.2	19.6 ± 3.4	.726
HBV DNA (log copies/mL)	4.5 ± 1.3	4.6 ± 1.3	4.3 ± 1.3	.317
HBsAg (log IU/mL)	3.1 ± 0.8	3.1 ± 0.8	3.1 ± 0.9	.651

NOTE. Data are expressed as mean ± SD.

^aP values in comparison between I97wt and I97L are indicated.

Table 2. Biochemical Markers of Patients With I97wt or I97L at the End of Observation

	Total (n = 77)	HBV-I97wt (n = 37)	HBV-I97L (n = 40)	P value ^a
Observation period (y)	7.2 ± 3.5	6.8 ± 4.0	7.6 ± 3.0	.325
ALT (IU/L)	31.3 ± 38.5	40.1 ± 38.9	23.1 ± 36.7	.052
Rate of ALT within the normal range achieved (<30 IU/L)	17/28 (60.7%)	6/15 (40.0%)	11/13 (84.6%)	.016
Gamma-glutamyl transpeptidase (IU/L)	24.6 ± 16.9	29.0 ± 21.1	20.5 ± 10.7	.033
HBV DNA (log copies/mL)	3.2 ± 2.0	4.0 ± 1.9	2.4 ± 1.9	<.0001
HBsAg (log IU/mL)	1.8 ± 2.1	2.4 ± 1.7	1.3 ± 2.3	.029
Reduction of HBV DNA (log copies/mL/y)	-0.24 ± 0.50	-0.12 ± 0.44	-0.36 ± 0.53	.030
Reduction of HBsAg (log IU/mL/y)	-0.19 ± 0.26	-0.12 ± 0.22	-0.25 ± 0.28	.029
Rate of HBV DNA undetectable (%)	23.4 (18/77)	10.8 (4/37)	35.0 (14/40)	.012
Rate of functional cure (%) (HBsAg undetectable)	18.2 (14/77)	8.1 (3/37)	27.5 (11/40)	.028

NOTE. Data are expressed as mean ± SD.

^aP values in comparison between I97wt and I97L are indicated.

Effects of I97L on Cell Culture-Generated HBV

The effects of I97L on the cell culture-generated HBV (HBVcc) were also evaluated. We introduced I97L into the replication-competent HBV genotype C molecular clone, and the clone generated (HBV-I97L) was compared with the genotype C wild-type molecular clone (HBV-I97wt). HBV-I97L and HBV-I97wt were transfected into HepG2 cells, and the production of HBV proteins and infectious viruses was assessed. The extracellular and intracellular HBsAg levels of HBV-I97L-transfected cells were similar to those of HBV-I97wt-transfected cells (Figure 4A, left). The extracellular HBcrAg level of HBV-I97L-transfected cells was significantly higher than that of HBV-I97wt-transfected cells, although intracellular HBcrAg levels of these clone-transfected cells were comparable (Figure 4A, middle). The extracellular HBV DNA level of HBV-I97L-transfected cells was significantly lower than that of HBV-I97wt-transfected cells (Figure 4A, right).

HBVcc of HBV-I97wt and HBV-I97L were also analyzed by iodixanol density gradient, applying the same amount of HBV DNA to compare the infectivity (Figure 4B and C). In the density gradients of HBV-I97wt and HBV-I97L, HBsAg peaked at fraction 13, but the HBsAg level in the peak fraction of HBV-I97L was higher than that of HBV-I97wt because of the presence of more HBsAg in the culture medium of HBV-I97L containing the same amount of HBV DNA. In these density gradients, HBcrAg exhibited 2 peaks at fractions 13 and 16. The ratio of the HBcrAg level in fraction 13 to fraction 16 was higher for HBV-I97L than HBV-I97wt, suggesting higher levels of envelope-interacted HBcrAg for HBV-I97L than HBV-I97wt. Because concentrated culture media containing the same amount of HBV DNA were applied to these density gradients, the HBV DNA titers in the 2 peaks were comparable (fractions 14 and 16 for HBV-I97wt and fractions 13 and 16 for HBV-I97L). When infected with the same volume of fractions, the peak infectivity was observed at fraction 14 for HBV-I97wt, and the number of HBV-positive cells was $4.83 \times 10^2 \pm 2.29 \times 10^1$. Similarly, fraction 14 of HBV-I97L showed the peak infectivity, and the number of HBV-positive cells was $1.64 \times 10^2 \pm$

2.36×10^1 , indicating approximately 3-fold lower infectivity than that of HBV-I97wt (Figure 4B and C, lower panel). The highest infectivity titers that normalized with GEq were observed at fraction 14 of HBV-I97wt (1.44×10^{-3} count/GEq) and at fraction 15 of HBV-I97L (3.89×10^{-4} count/GEq).

Effects of I97L on Interaction Between HBc and L-HBs

To confirm the efficient interaction between I97L-HBc and HBs proteins, we used the NanoLuc Binary Technology (NanoBiT). This system uses dissected NanoLuc into 2 components, Small BiT (SmBiT) and Large BiT (LgBiT). These 2 components have poor intrinsic affinity and strong conformational stability and create a split-reporter to assess the protein-protein interactions. The HBs protein consists of 3 species: small (S-), middle (M-), and large (L-) HBs, and the L-HBs protein is known to interact with HBc protein when assembling the viral particles. Thus, we prepared a plasmid of I97wt-HBc-LgBiT that expresses the fusion protein of HBc and LgBiT and a plasmid of SmBiT-L-HBs that expresses the fusion protein of SmBiT and L-HBs. The plasmid of I97L-HBc-LgBiT that expresses the fusion protein of HBc with the I97L substitution and LgBiT was also prepared. These plasmids were transfected with the plasmid of HBV1.4-fold [Δ HBe/c, Δ preS1] that expresses the HBV proteins other than HBc and L-HBs and also produces pre-genomic RNA (pgRNA) that acts as the HBV genome for encapsidation (Figure 5A). After transfection of these plasmids, the NanoLuc signal was generated by the interaction of HBc and L-HBs proteins. The NanoLuc signal generated by the interaction was significantly higher in the I97L-HBc-LgBiT transfected cells than that in the I97wt-HBc-LgBiT transfected cells (Figure 5B).

Detection of HBV DNA Species in Cell Culture-Generated HBV-I97wt and -I97L

To evaluate the underlying mechanisms of the difference in infectivity between these clones, we compared HBV DNA

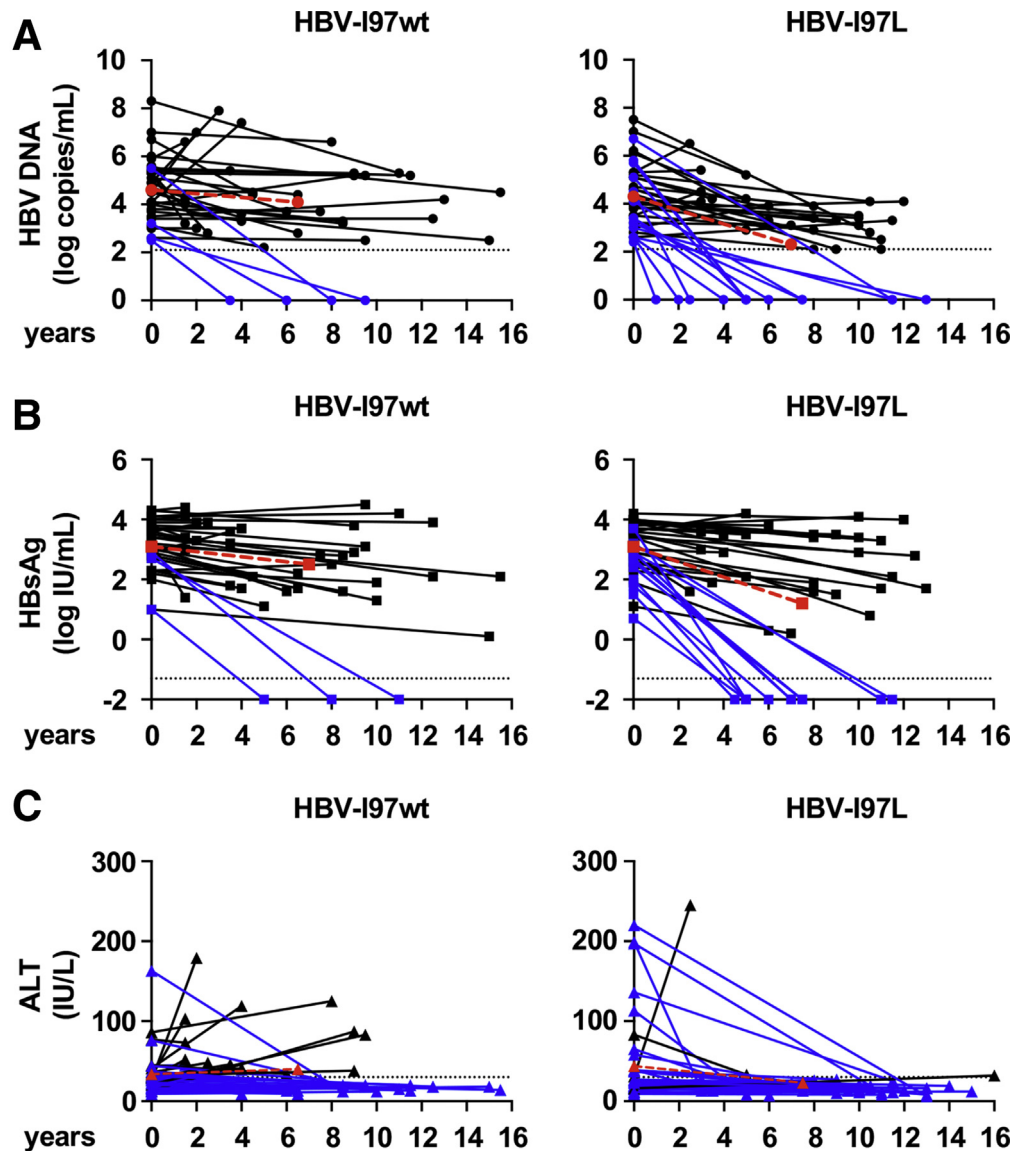


Figure 2. Transition of HBV DNA, HBsAg, and ALT in patients with HBV-I97wt or -I97L. (A) Transition of HBV DNA from the start to end of the observation period in patients with HBV-I97wt (*left*) or HBV-I97L (*right*). *Blue solid line* indicates patients who achieved undetectable level of HBV DNA during the observation period. *Red dashed line* indicates the average of the included patients. *Dotted line* indicates the lower detection limit of HBV DNA. (B) Transition of HBsAg from the start to the end of the observation period in patients with HBV-I97wt (*left*) or HBV-I97L (*right*). *Blue solid line* indicates patients who achieved undetectable level of HBsAg during the observation period. *Red dashed line* indicates the average of the included patients. *Dotted line* indicates the lower detection limit of HBsAg. (C) Transition of ALT from the start to the end of the observation period in patients with HBV-I97wt (*left*) or HBV-I97L (*right*). *Blue solid line* indicates patients who achieved within normal range of ALT during the observation period. *Red dashed line* indicates the average of the included patients. *Dotted line* indicates the normal range of ALT.

species in the fractions from iodixanol density gradients of HBV-I97wt and -I97L by Southern blotting (Figure 6A). In the density gradient of HBV-I97wt, the highest amount of relaxed-circular HBV DNA (RC) was detected in the peak fraction of infectivity (fraction 14); single-stranded HBV DNA (SS) was scarcely detected. The ratio of the band density of RC/SS in fraction 14 was 3.68. For the density gradient of HBV-I97L, the highest amount of RC was also detected in the peak fraction of HBV DNA (fraction 13), but

the ratio of the band density of RC/SS in fraction 13 was 1.33.

To confirm these observations, we measured the HBV DNA titer by real-time polymerase chain reaction (PCR) targeting different HBV regions (Figure 6B). Specifically, the HBV DNA titer in the HBV-I97wt and HBV-I97L density gradient fractions was examined by real-time PCR, with primer and probe sets targeting the HBc region (HBc set) and the HBx region (HBx set). If the plus-strand of HBV DNA

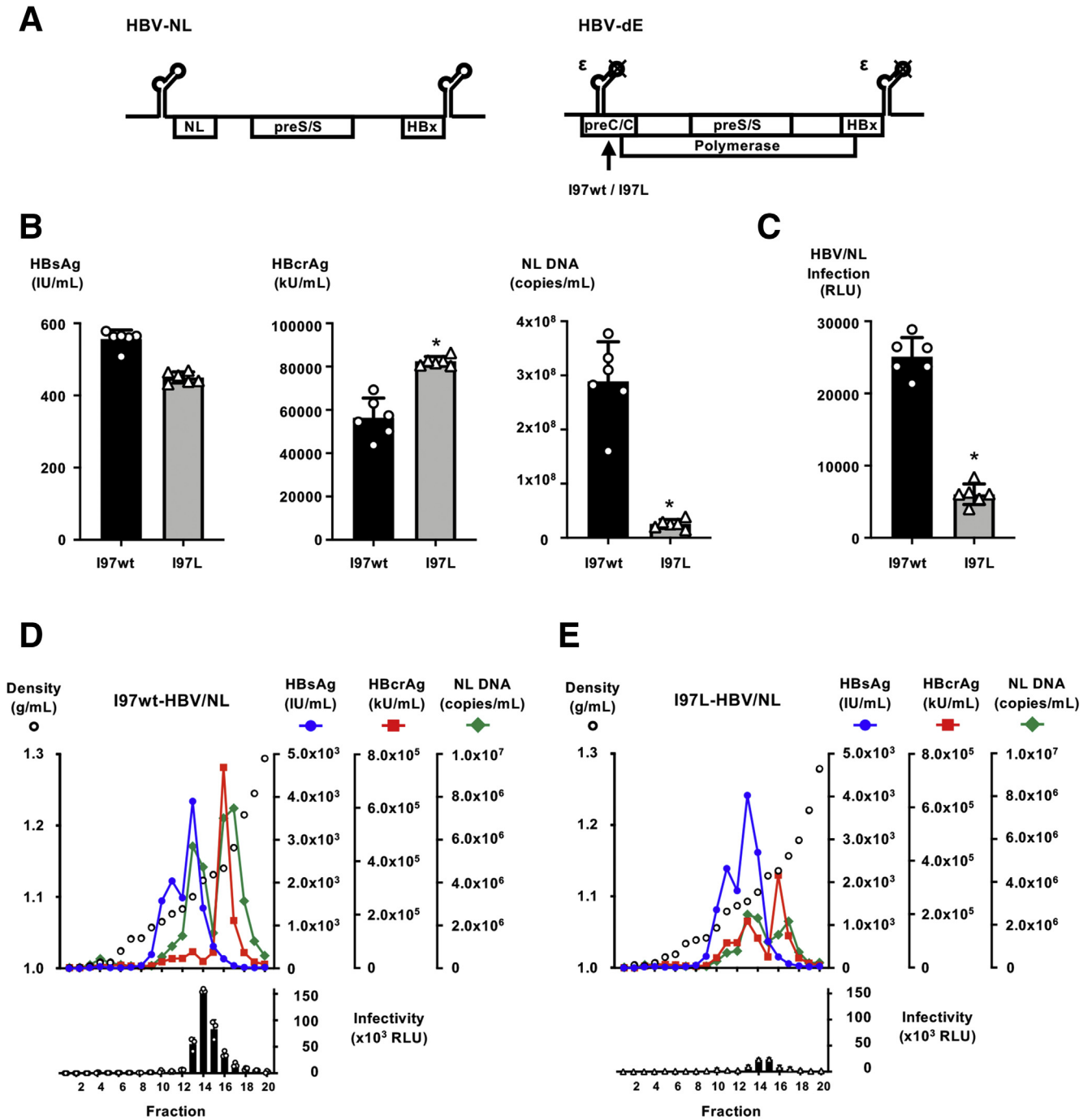


Figure 3. Effects of I97L substitution on HBV/NL infection. (A) Structure of plasmids for recombinant HBV reporter virus (HBV/NL). Constructs of encapsitation competent-reporter plasmid (HBV-NL) and encapsitation signal-lacking plasmid (HBV-dE). The amino acid substitution I97L was introduced into the HBV-dE plasmid. (B) Production of HBV proteins by transfection of plasmids for HBV/NL. Amounts of HBsAg, HBcrAg, and NL DNA in the culture medium were measured. Data represent the mean \pm SD of 6 experiments. * $P < .05$ in comparison with I97wt by *t* test. (C) Infection of I97wt- and I97L-HBV/NL. I97wt- and I97L-HBV/NL were infected into G2/NT18-C cells at 20 GEq/cell. After 8 days of incubation, the infected cells were lysed, and NL activities were measured. Data represent mean \pm SD of 6 experiments. * $P < .05$ in comparison with I97wt by *t* test. (D and E) Iodixanol density gradient analysis of cell culture-generated HBV-I97wt and HBV-I97L. I97wt-HBV/NL (D) and I97L-HBV/NL (E) were analyzed by iodixanol density gradient after adjusting amount of HBsAg. Titers of HBsAg and HBcrAg were measured in each fraction, and NL DNA was quantified by real-time PCR after treatment with DNase (*upper panel*). Infectivity of the generated HBV/NL was evaluated by the inoculation of the same volume of fractions into G2/NT18-C cells. Infected cells were lysed 8 days after infection, and NL activity was measured. Data represent mean \pm SD of triplicate (*lower panel*).

Table 3. Characteristics of I97wt- and I97L-HBV/NL in the Peak Fraction of Infectivity

Clone	I97wt-HBV/NL	I97L-HBV/NL	Ratio (I97wt/I97L)
Fraction	14	14	—
HBsAg (IU/mL)	1407.4	2696.0	0.52
HBcrAg (kU/mL)	24,000	111,620	0.22
NL DNA (copies/mL)	4.72×10^6	2.31×10^6	2.04
Infectivity (RLU)	$1.56 \times 10^5 \pm 3.14 \times 10^3$	$2.38 \times 10^4 \pm 1.16 \times 10^3$	6.55 ± 0.24
NL DNA-adjusted infectivity (RLU/copy)	165.0 ± 3.3	49.9 ± 5.4	3.33 ± 0.34

is synthesized, the HBV DNA titer measured with the HBc set is considered to be 2-fold higher than that measured with the HBx set. In the density gradient of HBV-I97wt, the amount of HBV DNA in the peak fraction of infectivity (fraction 14) was almost 2-fold higher when measured with the HBc set than that with the HBx set. This higher HBV DNA with the HBc set was also observed for the peak fraction of HBcrAg (fraction 16), but the ratio was approximately 1-fold (Figure 6C, left). On the other hand, in the density gradient of HBV-I97L, the amount of HBV DNA in both peak fractions of HBsAg (fraction 13) and HBcrAg (fraction 16) was higher when using the HBx set than the HBc set (Figure 6C, right).

Effects of I97L Substitution on cccDNA Synthesis

To assess the effects of I97L on the HBV life cycle, we evaluated the efficiency of each step in HBV infection. By using the purified viruses HBV-I97wt and -I97L, the efficiencies of the steps of attachment, internalization, and cccDNA synthesis were analyzed. The amounts of attached viruses on the cell surface and internalized viruses after incubation at 37°C were comparable between these clones (Figure 7A). However, the efficiency of cccDNA synthesis after infection with HBV-I97L was significantly lower than that after infection with HBV-I97wt (Figure 7B). We also assessed the efficiencies of cccDNA synthesis by HBV genome recycling, whereby the efficiencies of pgRNA transcription, encapsidation, reverse transcription (RT), and cccDNA recycling were evaluated after transfection of the HBV molecular clone. The efficiencies of pgRNA transcription were similar between the molecular clones of HBV-I97wt and -I97L (Figure 7C). However, the level of core-associated HBV DNA was significantly lower in the HBV-I97L-transfected cells than in HBV-I97wt-transfected cells when measured by real-time PCR with the HBs set (Figure 7D, left). We assessed the HBV DNA species of core-associated HBV DNA by Southern blotting and found a predominance of SS in I97L-transfected cells in comparison with I97wt-transfected cells (Figure 7D, middle). This difference was confirmed by real-time PCR with the HBc and HBx sets (Figure 7D, right). The ratio of HBc/HBx was significantly lower in I97L-transfected cells than that in I97wt-transfected cells. The efficiency of cccDNA synthesis in I97L-transfected cells was also substantially lower than that in I97wt-transfected cells (Figure 7E). Taken together, our data indicated that the amino acid substitution I97L is

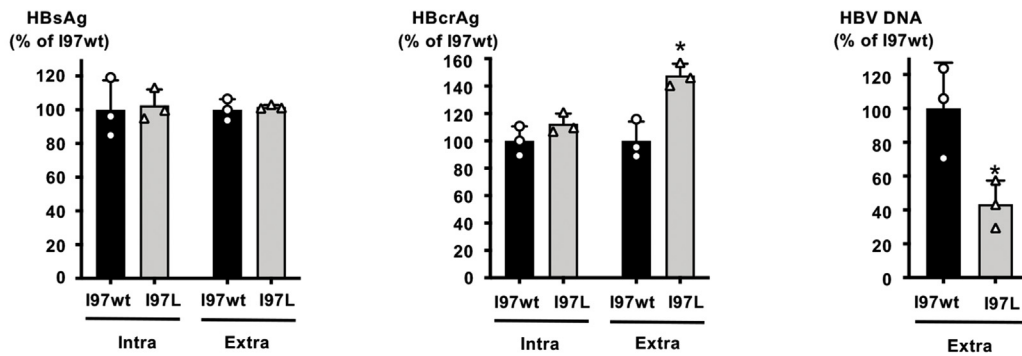
associated with the reduction of plus-strand HBV DNA synthesis and the production of immature virions with single-stranded DNA. As a result, the efficiency of cccDNA synthesis by infection and HBV genome recycling was hampered by this amino acid substitution (Figure 7F).

Discussion

The HBc protein constitutes the HBV nucleocapsid after interaction with pgRNA and HBV polymerase.^{17,18} Subsequently, the HBc protein comprising the nucleocapsid interacts with the L-HBs protein to form enveloped viral particles after maturation of the encapsidated HBV genome.^{19–22} This component of HBV particles has been suggested to be recognized by cytotoxic T lymphocytes,²³ and the HBc region is known to accumulate many amino acid substitutions in the natural course of chronic hepatitis.^{24–27} In our previous study, we found that the amino acid substitution I97L mainly emerges in HBeAg-negative patients and is associated with low HBV DNA, normal ALT, and HBsAg clearance.¹³ To date, this amino acid substitution, I97L, has been investigated in vitro.^{16,28–32} Yuan et al¹⁶ analyzed the cell culture-generated HBV-I97L virus by density gradient and demonstrated that this virus mainly contains a SS HBV DNA genome, even in the enveloped virion in the HBsAg-rich fraction, although the HBV-wt virus in the same fraction predominantly contains a RC HBV DNA genome. Recently, Wu et al³¹ investigated this amino acid substitution in vivo by using the mouse-hydrodynamic injection system of HBV molecular clones and suggested that HBV-I97L releases HBV virions with single-stranded genomes.³¹ They also indicated a lower amount of genomic DNA in hepatocytes and less persistence in the liver after hydrodynamic injection of the HBV molecular clone of HBV-I97L in comparison with HBV-wt, irrespective of the immune status of the mice. They used an HBV molecular clone that was HBeAg-positive in their study. The increase in the SS HBV DNA genome by the I97L substitution is suggested not to be restricted by the HBeAg status. Although the production of virions with immature single-stranded genomes by HBV-I97L has been demonstrated, the effects of this amino acid substitution on the clinical course of CHB and the HBV life cycle, especially for the infectivity of HBV-I97L or the synthesis of cccDNA, have not yet been clarified.

In this study, we used a cohort of HBeAg-negative patients with HBV-wt or -I97L. Sex, age, and clinical

A



B

C

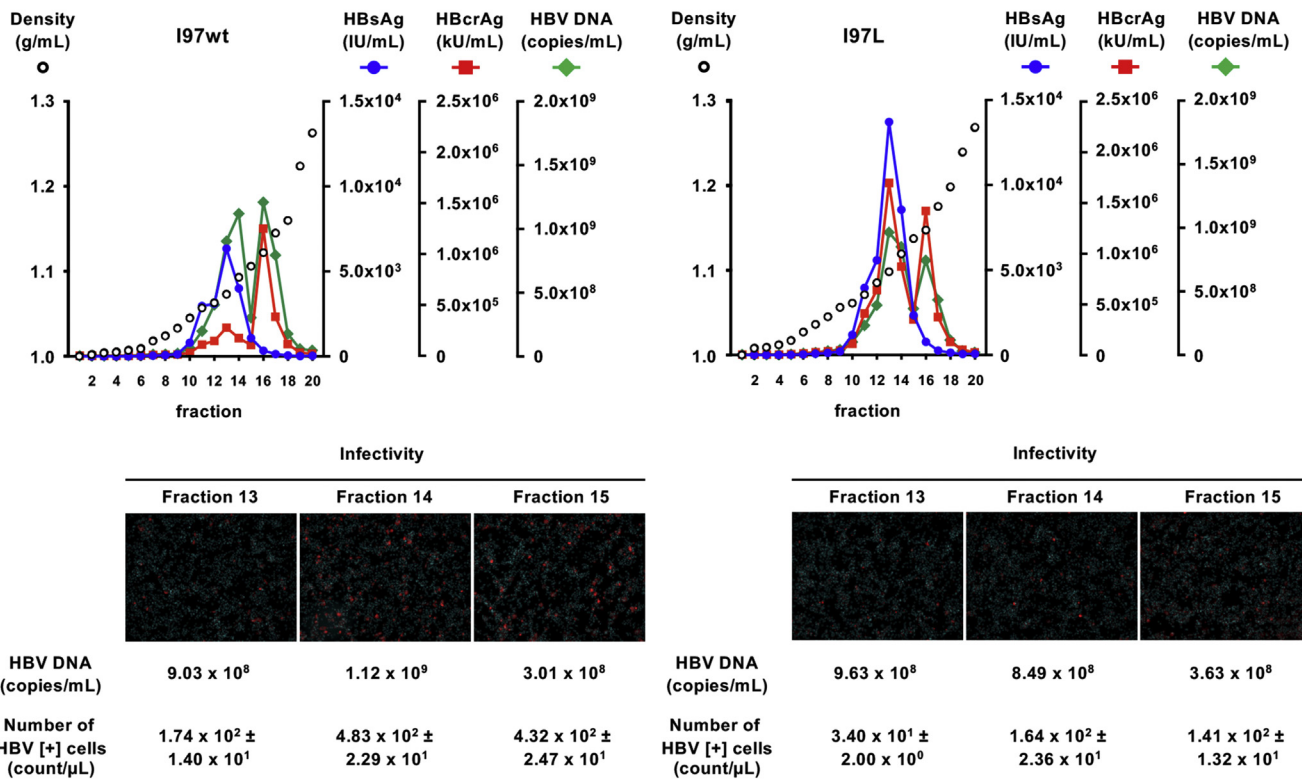


Figure 4. Effects of I97L substitution on HBV infection. (A) Amount of HBV proteins and HBV DNA after transfection of HBV molecular clone plasmids with I97wt or I97L. Extracellular and intracellular levels of HBsAg (left) and HBcrAg (middle) were measured. Extracellular level of HBV DNA was also measured by real-time PCR after DNase treatment (right). Data are shown relative to the production of HBV-I97wt-transfected cells and indicated as mean ± SD of triplicate. **P* < .05 in comparison with I97wt. (B and C) Iodixanol density gradient analysis of cell culture-generated HBV-I97wt and HBV-I97L. Culture medium of the HBV molecular clone with I97wt- or I97L-transfected cells was applied to iodixanol density gradient after adjusting amount of HBV DNA. Titers of HBsAg and HBcrAg were measured in each fraction, and HBV DNA was quantified by real-time PCR after DNase treatment (upper panel). Infectivity of cell culture-generated HBV in the indicated fractions was also evaluated by inoculation of the same volume of fractions onto HepG2/NTCP-sec+ cells (lower panel). Infected cells were fixed 12 days after infection. HBV-positive cells were visualized by staining with anti-HBc antibody (red), and nuclei were visualized by DAPI (blue). HBV DNA titer and number of HBV-positive cells (mean ± SD of triplicate) are indicated.

backgrounds were matched between the patients with HBV-wt and -I97L, and the mean observation periods for these groups were similar. At the end of the observation, the levels of HBsAg and HBV DNA were significantly lower in patients with HBV-I97L than in those with HBV-I97wt. A

higher rate of ALT within the normal range achieved was also detected in patients with HBV-I97L. The rates of undetectable HBsAg and HBV DNA and the mean annual reduction in these markers were also higher in patients with HBV-I97L than in those with HBV-I97wt. These

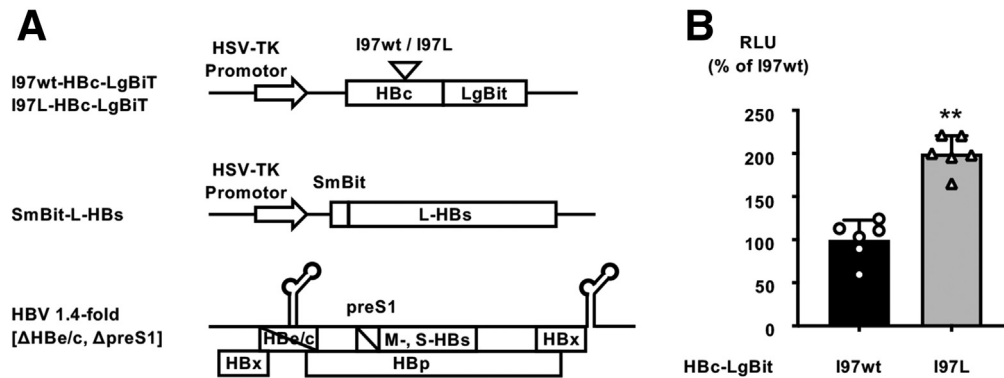


Figure 5. Effects of I97L substitution on interaction between HBc and L-HBs. (A) Structure of plasmids used in this assay. Expression plasmids for the fusion protein of HBc and LgBiT (HBc-LgBiT) and the fusion protein of SmBiT and L-HBs (SmBiT-L-HBs) were prepared. Two kinds of HBc-LgBiT harboring I97wt (I97wt-HBc-LgBiT) and I97L (I97L-HBc-LgBiT) were generated. The plasmid of HBV 1.4-fold [Δ HBe/c, Δ preS1] was generated by modifying the first methionine of ORFs of HBe, HBc, and preS1 regions to erase the expressions of HBe, HBc, and L-HBs proteins by using the HBV genotype C molecular clone. (B) NanoLuc signals produced by interaction between proteins of HBc-LgBiT and SmBiT-L-HBs. Amount of NanoLuc signals were measured after transfection of indicated 3 plasmids. Data represent mean \pm SD of 6 experiments. ** $P < .0001$ in comparison with I97wt by t test.

observations were consistent with our previous data for CHB,¹³ and they also agree with the *in vivo* observations in mouse models reported by other researchers.³¹ Chua et al³³ reported the infection of mixed I97 species in HBeAg-positive or -negative patients, although such mixture was detected in only 4 patients in this study and it has minimum impacts on clinical features. The compensatory substitutions of amino acid at 5 and 130 have also been reported to improve the immature secretion phenotype by the I97L substitution.^{34,35} More study will be needed for the clinical features of patients with the mixed I97 species and the compensatory substitutions.

Moreover, we assessed the effects of the emergence of I97L in the HBV genome on the HBV life cycle by using an *in vitro* HBV infection system and found that introduction of I97L in the HBc region reduces the infectivity of HBV. In the HBV reporter virus infection system, the luciferase activity in I97L-HBV/NL-infected cells was lower than that in I97wt-HBV/NL-infected cells, even after infection with virus adjusted by the NL DNA level. In addition, iodixanol density gradient analysis revealed that the profile patterns of HBsAg, HBcrAg, and NL DNA were similar between I97L-HBV/NL and I97wt-HBV/NL, although the rate of HBc protein coexisting with HBsAg was higher in I97L-HBV/NL than in I97wt-HBV/NL. Luciferase activity after infection of the peak fraction of infectivity was lower for I97L-HBV/NL than for I97wt-HBV/NL. The difference in infectivity between the peak fractions of I97wt- and I97L-HBV/NL was almost identical to that of the difference in infectivity of unpurified culture media. These data indicate that the lower infectivity of I97L-HBV/NL can be attributed to the infectivity of the viruses generated and not to the efficiencies of encapsidation or envelopment of the virion. This lower infectivity of HBV with I97L was also confirmed by infection of HBVcc. The number of HBc-positive cells by infection of the peak fraction of HBV-I97L infectivity was approximately 3-fold

lower than that of HBV-I97wt, even though the HBV DNA levels were comparable.

By Southern blotting analysis, we detected the release of immature HBV particles with a single-stranded genome from HBV-I97L-transfected cells, as reported by other researchers. This production of an immature HBV genome was also confirmed by ratios of HBV DNA titers quantified by real-time PCR with primer and probe sets targeting the HBc and HBx regions. We reasoned that the production of immature particles is associated with lower infectivity of HBV-I97L and assessed the step of the HBV life cycle affected by this substitution. The efficiencies of attachment and internalization by infection after adjusting the HBV DNA titers of cell culture-generated HBV-I97wt and -I97L viruses were comparable. However, the efficiency of cccDNA synthesis by infection with HBV-I97L was significantly lower than that of HBV-I97wt. These data imply that HBV-I97L containing a single-stranded genome can attach to the cell and invade as well as HBV-wt can, but HBV-I97L cannot synthesize cccDNA at a similar level after internalization. We also evaluated the efficiency of cccDNA recycling by the transfection of HBV molecular clones. The production efficiency of core-associated HBV DNA was lower in HBV-I97L-transfected cells than in HBV-I97wt-transfected cells, but the transcription level of pgRNA was comparable. The predominance of the single-stranded genome in HBV-I97L-transfected cells was confirmed by Southern blotting, and the amounts of HBV DNA were quantified by targeting HBc and HBx regions. The amount of cccDNA generated by the recycling of encapsidated HBV DNA was also lower in HBV-I97L-transfected cells than in HBV-I97wt-transfected cells. Taken together, our *in vitro* data clearly indicated that the production level of cccDNA by either infection or recycling was reduced in HBV-I97L. This reduction in the efficiency of cccDNA synthesis by HBV-I97L can explain the *in vivo* data of the low amount of genomic DNA in

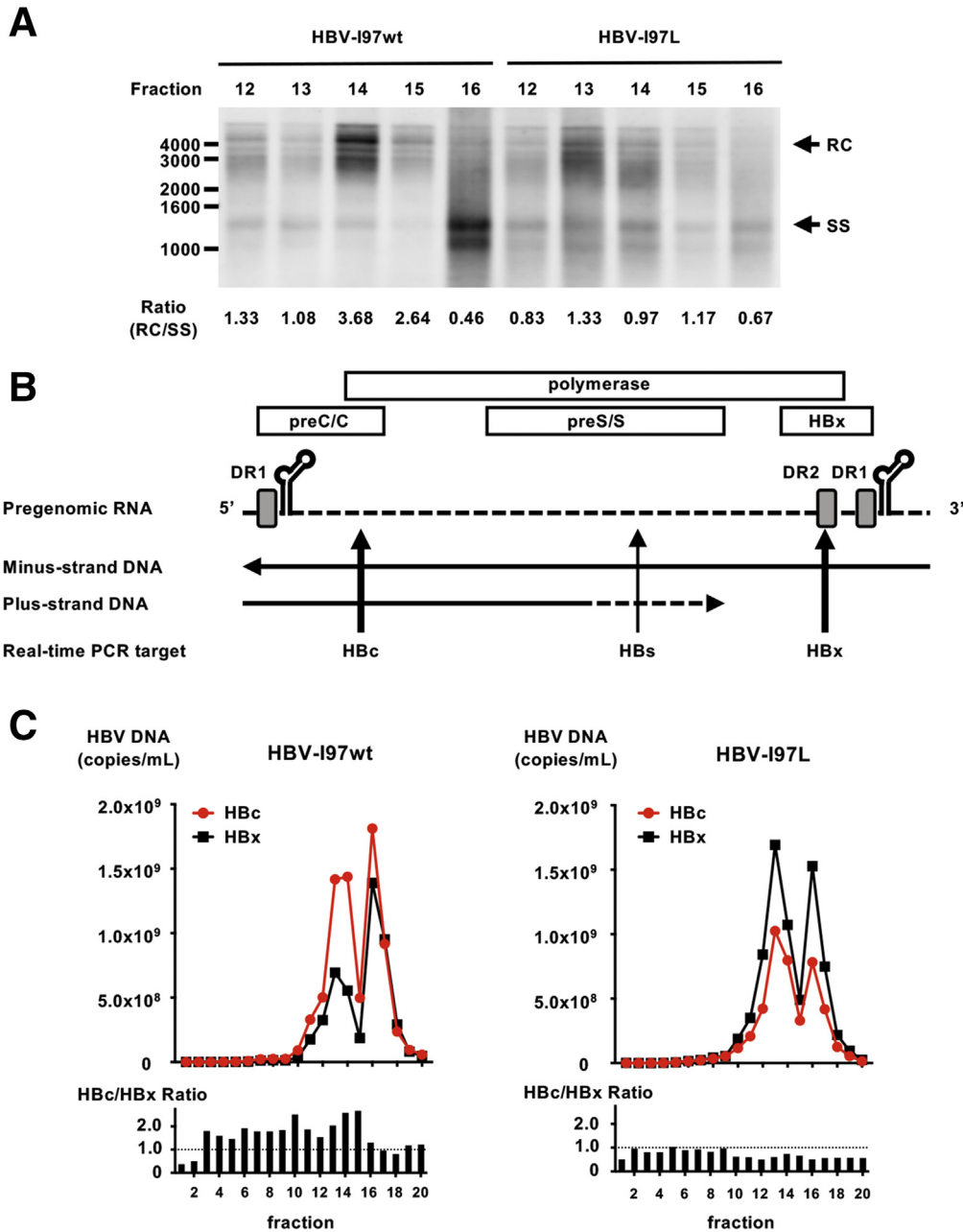


Figure 6. Detection of HBV DNA species in fractions of density gradients. (A) Southern blot analysis of HBV DNA species in fractions of iodixanol density gradients of HBV-I97wt and -I97L. Total DNA was extracted from indicated fractions of iodixanol density gradient, and HBV DNA was detected by Southern blotting hybridization. Ratios of densities of relaxed-circular HBV DNA (RC) and single-stranded HBV DNA (SS) are indicated at bottom of the blot. (B) Schematic presentation of targets of the primer and probe sets for real-time PCR used in this study. Encoded regions of the HBV genome, the structure of pregenomic RNA, and the length of minus- and plus-strand HBV DNA are indicated. Position of the primer and probe sets is also specified at the bottom. The 3' end of synthesized plus-strand HBV DNA varies. (C) HBV DNA titers quantified by real-time PCR with the primer and probe set targeting the HBc and HBx regions. Ratio of quantified values by the primer and probe sets of HBc and HBx is indicated at the bottom.

hepatocytes or reduced persistence in the liver after hydrodynamic injection of the HBV-I97L molecular clone into mice, as indicated by other researchers, and the high rate of undetectable HBsAg and HBV DNA and the high annual reduction of these markers in HBV-I97L-infected patients in our clinical observation.

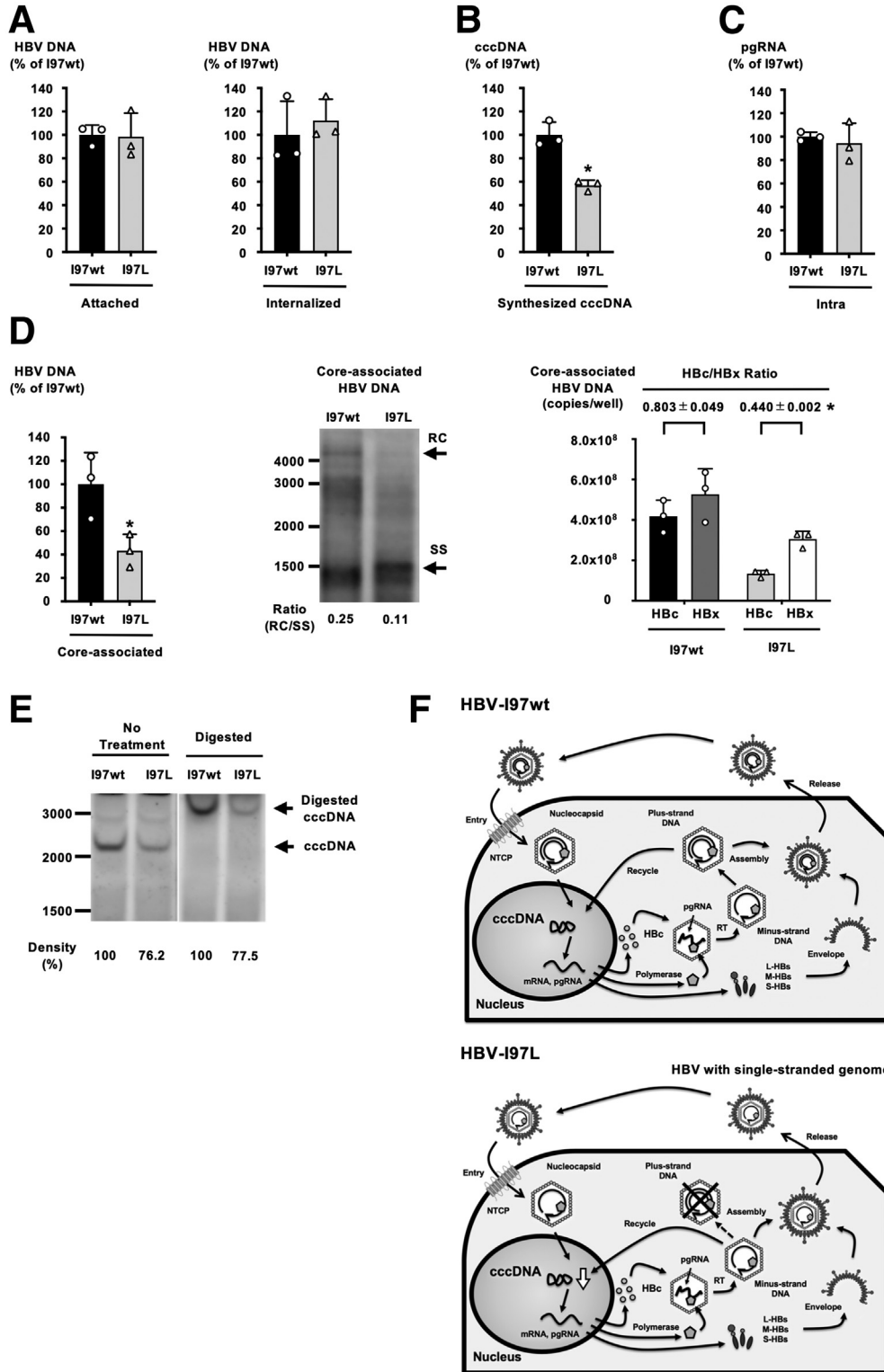
The mechanisms of I97L-dependent predominance of the single-stranded genome are still obscure. The amino acids isoleucine and leucine are structurally similar, and both are hydrophobic. Substitution of these amino acids would seem not to affect the HBV life cycle. However, we and other researchers found that HBV-I97L predominantly generates immature virions with the single-stranded genome, whereas HBV-I97wt preferentially generates mature virions with the

partially double-stranded relaxed-circular genome.¹⁶ This observation may suggest that the completion of synthesis of the mature relaxed-circular genome affects the structure of capsids and provides a signal for envelopment and/or virion secretion. The amino acid substitution I97L may be associated with modification of this signal. In our density gradient analysis of cell culture-generated HBV-I97L, we detected the predominant coexistence of HBc and HBs proteins. The capsid with the I97L substitution may have a high affinity for envelope proteins and easily be able to interact with the L-HBs protein contained in the envelope. The higher affinity of HBc protein with I97L to L-HBs protein compared with that of HBc protein with I97wt was confirmed by a split-reporter system for the protein-protein interactions. The

involvement of the hydrophobic pocket around this amino acid with virion secretion has been reported, and a difference in the size of this pocket between wild-type virions and a strain with amino acid substitution at this position has

been identified.³⁶⁻³⁸ Further investigation will be needed to associate the size of the pocket and the HBc-HBs interaction.

In conclusion, we found that the amino acid substitution I97L in the HBc region is associated with stable hepatitis



characterized by ALT within the normal range and undetectable levels of HBsAg and HBV DNA. This amino acid substitution leads to low efficiency of cccDNA synthesis by both infection and recycling via the production of an immature virion with a single-stranded genome.

Materials and Methods

All authors had access to the study data and had reviewed and approved the final manuscript.

Patients

Serum samples were collected from CHB patients who were outpatients of Nagoya University Hospital from April 2002 to October 2017 after obtaining written informed consent. We obtained samples from 183 consecutive patients infected with HBV genotype C. None of the patients had concomitant liver diseases such as fatty liver, hepatitis C virus, or alcohol use. Among them, 77 HBeAg-negative patients were enrolled in this study. The detailed inclusion and exclusion criteria are indicated in Figure 1. Once patients started the treatment with NA or IFN, the observation was terminated at that time. This study was approved by the Ethics Committees of our institutes (the approval numbers are 2017-0377 for Nagoya University Hospital and 770 for National Institute of Infectious Diseases).

Virologic Markers

The HBV genome sequence of the HBc region at the vicinity region around amino acid at 97 was determined by direct sequencing, as reported previously, by using patient serum obtained at baseline.¹³ The HBV DNA titer was measured by COBAS AmpliPrep/COBAS TaqMan HBV Test v2.0 (Roche Diagnostics, Tokyo, Japan). The dynamic range of this assay is 2.1–9.0 log copies/mL. The titers of HBsAg (Architect HBsAg QT; Abbott Japan, Tokyo, Japan), HBeAg

(Architect HBeAg; Abbott Japan), and anti-HBe (Architect HBeAb; Abbott Japan) were examined using chemiluminescence immunoassays. The lower detection limit of HBsAg is 0.05 IU/mL.³⁹

Cell Culture

HepG2 cells were obtained from the European Collection of Authenticated Cell Cultures (catalog #85011430; ECACC, Salisbury, UK) and kept in modified Eagle medium supplemented with 10% fetal calf serum. Sodium taurocholate cotransporting polypeptide-transduced HepG2 cells HepG2/NTCP-C4,⁴⁰ HepG2-NTCPsec+,⁴¹ and G2/NT18-C⁴² were used as described previously.^{15,43}

Replication-Competent HBV Molecular Clones

A replication-competent HBV clone with a 1.38-fold genome length was constructed by using the genome sequence of HBV.^{15,44} In this study, we used the HBV genotype C clone (accession number AB246344).^{15,45} This clone has the amino acid substitution G1896A, which prevents HBeAg production. The I97L substitution was introduced by site-directed PCR and fragment swapping.⁴⁴ Lipofectamine 3000 Reagent (catalog #L3000015; Thermo Fisher Scientific, Waltham, MA) was used for transfection of the HBV molecular clone plasmids. The transfected cells and HBV in the culture medium were harvested 1 week after transfection. The collected media were stored after passing through a 0.45- μ m filter to remove cell debris. The intracellular and extracellular levels of HBsAg were measured by chemiluminescent enzyme immunoassay using commercial assay kits (Lumipulse; Fujirebio, Tokyo, Japan).³⁹ The intracellular and extracellular levels of HBcrAg consisting of 3 proteins (HBcrAg consists of HBV particles, HBeAg, and a 22-kDa precore protein) encoded by the precore/core region were also measured by chemiluminescent enzyme immunoassay with commercial assay kits.⁴⁶

Figure 7. (See previous page) Effects of I97L substitution on the HBV life cycle. Efficiencies of attachment and internalization of purified HBV-I97wt and -I97L viruses. Viruses were purified by density gradient, treated with DNase, and attached to the surface of HepG2/NTCP-C4 cells at 4°C for 3 hours without PEG8000 at 50 GEq/cell. Then, the viruses were internalized by moving the virus-attached cells to 37°C. The cells were harvested at each step, and HBV DNA was measured by real-time PCR. Data are shown relative to HBV-I97wt-infected cells and represent mean \pm SD of triplicate. (B) Efficiencies of cccDNA synthesis after infection with HBV-I97wt and -I97L. Viruses were purified by density gradient, treated with DNase, and used to infect HepG2/NTCP-C4 cells at 500 GEq/cell. The synthesized cccDNA was evaluated at 12 days after infection. Data represent mean \pm SD of triplicate. * $P < .05$ in comparison with I97wt by t test. (C) Transcription of pgRNA after transfection of HBV molecular clone plasmids carrying I97wt and I97L. These plasmids were transfected into HepG2 cells, and the transcribed pgRNA was measured. Data are shown relative to HBV-I97wt-transfected cells. (D) Detection of core-associated DNA in I97wt and I97L HBV molecular clone plasmid-transfected HepG2 cells. Amounts of core-associated DNA were measured by real-time PCR (*left panel*). Data are shown relative to HBV-I97wt-transfected cell production and represent mean \pm SD of triplicate. * $P < .05$ in comparison with I97wt by t test. HBV DNA species of core-associated DNA was detected by Southern blot analysis (*middle panel*). Ratios of densities of relaxed-circular HBV DNA (RC) and single-stranded HBV DNA (SS) are indicated at bottom of the blot. HBV DNA titers of core-associated DNA were quantified by real-time PCR with primer and probe sets targeting HBc and HBx regions (*right panel*). Data represent mean \pm SD of triplicate. Ratio of quantified values by HBc/HBx sets is indicated at the top. * $P < .05$ in comparison with I97wt by t test. (E) Synthesis of cccDNA after transfection of HBV molecular clone plasmids with I97wt and I97L. Transfected cells were harvested 7 days after transfection, and synthesized cccDNA was detected by Southern blotting hybridization after Hirt extraction. The XbaI digested sample was also applied. Density of cccDNA bands is indicated at the bottom. (F) The points of the HBV life cycle affected by I97L. The schemes of the HBV-I97wt (*left*) and HBV-I97L (*right*) life cycles are indicated. *White down arrow* in the right panel indicates the reduction in cccDNA synthesis. L-HBs, large HBs; M-HBs, middle HBs; S-HBs, small HBs.

Recombinant HBV Reporter Virus System

The recombinant HBV reporter virus (HBV/NL) infection system was exploited to assess HBV infection.^{14,15} This system uses 2 plasmids, HBV-NL (originally designated pUC1.2xHBV/NL encoding the 1.2-fold HBV genome replacing precore/core and a part of polymerase with NL) and HBV-dE (originally designated pUC1.2xHBV-D encoding the 1.2-fold HBV genome lacking the encapsidation signal) (Figure 3A). By transfection of these plasmids, HBV/NL harboring the NL gene as a reporter was generated and secreted into the culture medium. After infection of generated HBV/NL, HBV infection can be monitored by measuring the NL activities of the infected cells. We constructed HBV-NL and HBV-dE plasmids with the HBV genotype C clone (accession number AB246344). HBV-dE with I97L was generated by site-directed PCR and fragment swapping using appropriate restriction enzymes.⁴⁴ These plasmids were transfected into HepG2 cells with Lipofectamine 3000 Reagent. HBV/NL in the culture medium was harvested 1 week after transfection, and the viral titer was measured by real-time PCR with a primer and probe set after treatment with DNase (RQ1 RNase-Free DNase, catalog #M6101; Promega, Madison, WI).¹⁵ HBV/NL infection was assessed by measuring luciferase activity in infected G2/NT18-C cells using a Nano-Glo Luciferase Assay System (catalog #N1130; Promega) after lysis of the infected cells with Passive Lysis Buffer (catalog #E1941; Promega). The levels of HBsAg and HBcAg were also measured by chemiluminescent enzyme immunoassay using commercial assay kits.

Iodixanol Density Gradient Analysis

HBVcc was purified with a HiTrap heparin HP Column (catalog #17040703; GE Healthcare, Chicago, IL),⁴⁷ concentrated with Amicon Ultra centrifugal filter units (100 kDa, catalog #UFC910096; Merck Millipore, Tullagreen, Ireland), and analyzed by iodixanol density gradient (10%–40%) centrifugation at 38,000 rpm for 16 hours at 4°C in an SW 41 Ti rotor. Fractions were collected from the top of the gradient, and the density and HBsAg and HBcAg titers were measured for each fraction. Alternatively, the HBV DNA titer was measured by real-time PCR targeting HBs (primers: HBSF2: CTTCATCTGCTGCTATGCCT and HBSR2: AAAGCCCAG GATGATGGGAT; probe: HBSP2: ATGTTGCCCGTTTGTCTCTAATTCCA),⁴⁸ HBc (primers: HBCF1: AGTGTGGATTTCGACTCCT and HBCR1: GAGTCTTCT TCTAGGGGACCTG; probe: HBCP1: CCAAATGCCCTATCT-TATCAACACT TCC),⁴⁹ or HBx (primers: HBXF1: ACGTCCTTTGTTTACGTCCCGT and HBXR1: CCCAACTCTCC-CAGTCCTTAA; probe: HBXP1: TGTCACGACCGACCT TGAGG-CATA)⁴⁸ regions after treatment with DNase. To assess HBVcc infection, the collected fraction was inoculated onto HepG2/NTCP-C4 cells in the presence of 4% PEG8000 and 2% dimethyl sulfoxide (catalog #09659-14; Nacal Tesque, Kyoto, Japan) for 16 hours. The infected cells were visualized by staining with rabbit polyclonal anti-HBc antibody (Ab-1, catalog #RB-1413-A; Thermo Fisher Scientific) and Alexa Fluor 555-conjugated anti-rabbit immunoglobulin G (catalog #A32732; Thermo Fisher Scientific). Detection with the

anti-HBc antibody was confirmed not to be affected by the I97L substitution (data not shown). Nuclei were stained with 4',6-diamidino-2-phenylindole (DAPI).

NanoBiT System for Interaction Between HBc and L-HBs Proteins

The NanoBiT PPI Starter System (catalog #N2014; Promega) was used for the detection of interaction between HBc and L-HBs proteins. To generate the HBc-LgBiT plasmid, the HBc region of HBV genotype C (accession number AB246344) was amplified by PCR with appropriate primers and inserted into pBiT1.1-C after digestion with EcoRI and XhoI (Figure 5A). To generate the SmBiT-L-HBs plasmid, the L-HBs region of the same HBV clone was amplified by PCR with appropriate primers and inserted into pBiT2.1-N after digestion with XhoI and EcoRI. The HBV 1.4-fold [Δ HBe/c, Δ preS1] plasmid was also generated by modifying the first methionine of ORFs of HBe, HBc, and preS1 regions to erase the expression of HBe, HBc, and L-HBs proteins of the replication-competent HBV genotype C molecular clone. The addition of this plasmid to the plasmids for the expression of HBc and L-HBs proteins enables the enhancement of the interaction signal by mimicking the assembly of viral particles. The intracellular NanoLuc signal generated by the interaction between LgBiT and SmBiT was quantified 3 days after transfection.

Isolation of Core-Associated HBV DNA

Intracellular core-associated HBV DNA was isolated by the method described by Günther et al⁵⁰ with some modifications.⁴⁴ Briefly, cells were suspended in 500 μ L of lysis buffer (100 mmol/l Tris-HCl [pH 8.0], 0.2% NP-40), and nuclei were pelleted by centrifugation. The supernatant was transferred and treated with DNase (RQ1 RNase-free DNase; Promega) and RNase (RNase A; Qiagen K.K.). Then, proteinase K, 500 mmol/L EDTA, 5 mol/L NaCl, and 10% sodium dodecyl sulfate (SDS) were added, and the samples were incubated at 55°C for 1 hour. Then, HBV DNA was recovered by phenol-chloroform (1:1) extraction and 2-propanol precipitation. The amount of core-associated HBV DNA was detected by Southern blot hybridization or measured by real-time PCR with the described primer and probe sets.^{44,48,49}

Southern Blot Hybridization of HBV DNA

The intracellular core-associated HBV DNA or HBV DNA in the collected iodixanol density gradient fractions was separated on a 1.0% agarose gel and transferred to a nylon membrane.⁴⁴ The DNA was immobilized on the membrane by UV crosslinking and hybridized with an alkaline phosphatase-labeled probe generated by the Gene Images AlkPhos Direct labeling kit (DIG-High Prime DNA Labeling and Detection Starter Kit II, catalog #11585614910; Roche Diagnostics, Mannheim, Germany) with a full-length HBV genotype C that was used for the construction of the replication-competent HBV clone. Chemiluminescence was detected by using the CDP-Star chemiluminescent substrate and analyzed with an Amersham Imager 680 (GE Healthcare

Japan, Tokyo, Japan). The ratios of RC HBV DNA and SS HBV DNA were calculated using built-in software.

Attachment and Internalization Assay

The attachment and internalization of HBV were evaluated by inoculating HBVcc purified by iodixanol density gradient. The viruses were attached to HepG2/NTCP-C4 cells at 50 GEq per cell at 4°C without PEG8000. After 3 hours of incubation, the attached viruses were harvested with Cell Lifter (catalog #3008; Corning, Corning, NY) after extensive washing to remove the residual inoculum. To assess virus internalization, the virus-attached cells were incubated at 37°C for 16 hours, and the amounts of attached and internalized viruses were measured by real-time PCR targeting the HBs region⁴⁸ after extraction of DNA with a QIAamp DNA Mini Kit (catalog #51306; Qiagen, Hilden, Germany).

Detection of cccDNA

cccDNA was extracted from HBV-infected cells by the Hirt protein-free DNA extraction procedure.⁵¹ The cells were treated with SDS and mixed with a high concentration of NaCl to precipitate high-molecular-weight cellular chromatin and protein bound to DNA. The supernatant containing cccDNA was collected after centrifugation, and phase extracted phenol and phenol-chloroform (1:1). cccDNA in the aqueous phase was precipitated by ethanol precipitation. The isolated cccDNA was treated with the Plasmid-safe ATP-dependent DNase (catalog #E3101K; Epicentre, Madison, WI). The titer of cccDNA was measured by real-time PCR with a cccDNA-specific primer and probe set (primers: C3F2: CGTCTGTGCCT TCTCATCTGC and C3R4: GCACAGCTTGGAGGCTTGAA; probe; C3P2: CTGTAGGCA-TAAATTGGT).⁵² For the transfection study of HBV molecular clones, the amount of cccDNA was evaluated by Southern blotting. To confirm the size of cccDNA, the digested samples with XbaI (catalog #R0145; New England Biolabs, Ipswich, MA) were also detected.

Detection of Pregenomic RNA

Total RNA was extracted from HBV-infected cells by using RNeasy Mini Kit (catalog #74106; Qiagen) with on-column DNase digestion (RNase-Free DNase set, catalog #79254; Qiagen). The extracted RNA was treated again with TURBO DNase (catalog #AM2239; Thermo Fisher Scientific) and further purified with RNeasy Mini Kit. cDNA was synthesized with Superscript VILO cDNA Synthesis Kit (catalog #11754-250; Thermo Fisher Scientific). HBV pgRNA was quantified by real-time PCR with a primer-probe set targeting the Hbc region.⁴⁹

Statistical Analysis

Key experiments were performed in triplicate, and the results are expressed as mean \pm standard deviation (SD). Differences between groups were determined by Student *t* test, and nonparametric data were analyzed by Welch's

correction. Differences in proportions were tested by χ^2 test. Statistical analyses were performed by using SPSS software, version 26 (SPSS Japan, Tokyo, Japan) or GraphPad PRISM 8 software (GraphPad Software, La Jolla, CA). *P* values were two-tailed, and *P* values $<.05$ were considered to be statistically significant.

References

1. Graber-Stiehl I. The silent epidemic killing more people than HIV, malaria or TB. *Nature* 2018;564:24–26.
2. Liang TJ, Block TM, McMahon BJ, Ghany MG, Urban S, Guo JT, Locarnini S, Zoulim F, Chang KM, Lok AS. Present and future therapies of hepatitis B: from discovery to cure. *Hepatology* 2015;62:1893–1908.
3. Nassal M. HBV cccDNA: viral persistence reservoir and key obstacle for a cure of chronic hepatitis B. *Gut* 2015;64:1972–1984.
4. Yim HJ, Lok AS. Natural history of chronic hepatitis B virus infection: what we knew in 1981 and what we know in 2005. *Hepatology* 2006;43(Suppl 1):S173–S181.
5. Lok AS, Zoulim F, Dusheiko G, Ghany MG. Hepatitis B cure: from discovery to regulatory approval. *J Hepatol* 2017;67:847–861.
6. Terrault NA, Lok ASF, McMahon BJ, Chang KM, Hwang JP, Jonas MM, Brown RS Jr, Bzowej NH, Wong JB. Update on prevention, diagnosis, and treatment of chronic hepatitis B: AASLD 2018 hepatitis B guidance. *Hepatology* 2018;67:1560–1599.
7. Fanning GC, Zoulim F, Hou J, Bertoletti A. Therapeutic strategies for hepatitis B virus infection: towards a cure. *Nat Rev Drug Discov* 2019;18:827–844.
8. Lok AS, Lai CL, Wu PC, Leung EK, Lam TS. Spontaneous hepatitis B e antigen to antibody seroconversion and reversion in Chinese patients with chronic hepatitis B virus infection. *Gastroenterology* 1987;92:1839–1843.
9. Lai CL, Chien RN, Leung NW, Chang TT, Guan R, Tai DI, Ng KY, Wu PC, Dent JC, Barber J, Stephenson SL, Gray DF. A one-year trial of lamivudine for chronic hepatitis B: Asia Hepatitis Lamivudine Study Group. *N Engl J Med* 1998;339:61–68.
10. Hadziyannis SJ, Tassopoulos NC, Heathcote EJ, Chang TT, Kitis G, Rizzetto M, Marcellin P, Lim SG, Goodman Z, Wulfsohn MS, Xiong S, Fry J, Brosgart CL; Adefovir Dipivoxil 438 Study G. Adefovir dipivoxil for the treatment of hepatitis B e antigen-negative chronic hepatitis B. *N Engl J Med* 2003;348:800–807.
11. Ghany MG, Doo EC. Antiviral resistance and hepatitis B therapy. *Hepatology* 2009;49(Suppl):S174–S184.
12. Wong GL, Seto WK, Wong VW, Yuen MF, Chan HL. Review article: long-term safety of oral anti-viral treatment for chronic hepatitis B. *Aliment Pharmacol Ther* 2018;47:730–737.
13. Honda T, Ishigami M, Ishizu Y, Kuzuya T, Hayashi K, Ishikawa T, Murakami Y, Iwadate M, Umeyama H, Toyoda H, Kumada T, Katano Y, Goto H, Hirooka Y. Core I97L mutation in conjunction with P79Q is associated with persistent low HBV DNA and HBs antigen clearance

- in patients with chronic hepatitis B. *Clin Microbiol Infect* 2017;23:407 e1–407 e7.
14. Nishitsuji H, Ujino S, Shimizu Y, Harada K, Zhang J, Sugiyama M, Mizokami M, Shimotohno K. Novel reporter system to monitor early stages of the hepatitis B virus life cycle. *Cancer Sci* 2015;106:1616–1624.
 15. Murayama A, Yamada N, Osaki Y, Shiina M, Aly HH, Iwamoto M, Tsukuda S, Watashi K, Matsuda M, Suzuki R, Tanaka T, Moriishi K, Suzuki T, Nishitsuji H, Sugiyama M, Mizokami M, Shimotohno K, Wakita T, Muramatsu M, Liang TJ, Kato T. N-terminal PreS1 sequence regulates efficient infection of cell-culture-generated hepatitis B virus. *Hepatology* 2021;73:520–532.
 16. Yuan TT, Tai PC, Shih C. Subtype-independent immature secretion and subtype-dependent replication deficiency of a highly frequent, naturally occurring mutation of human hepatitis B virus core antigen. *J Virol* 1999;73:10122–10128.
 17. Bartenschlager R, Junker-Niepmann M, Schaller H. The P gene product of hepatitis B virus is required as a structural component for genomic RNA encapsidation. *J Virol* 1990;64:5324–5332.
 18. Junker-Niepmann M, Bartenschlager R, Schaller H. A short cis-acting sequence is required for hepatitis B virus pregenome encapsidation and sufficient for packaging of foreign RNA. *EMBO J* 1990;9:3389–3396.
 19. Ueda K, Tsurimoto T, Matsubara K. Three envelope proteins of hepatitis B virus: large S, middle S, and major S proteins needed for the formation of Dane particles. *J Virol* 1991;65:3521–3529.
 20. Bruss V, Ganem D. The role of envelope proteins in hepatitis B virus assembly. *Proc Natl Acad Sci U S A* 1991;88:1059–1063.
 21. Poisson F, Severac A, Hourieux C, Goudeau A, Roingeard P. Both pre-S1 and S domains of hepatitis B virus envelope proteins interact with the core particle. *Virology* 1997;228:115–120.
 22. Bottcher B, Tsuji N, Takahashi H, Dyson MR, Zhao S, Crowther RA, Murray K. Peptides that block hepatitis B virus assembly: analysis by cryomicroscopy, mutagenesis and transfection. *EMBO J* 1998;17:6839–6845.
 23. Penna A, Bertoletti A, Cavalli A, Valli A, Missale G, Pilli M, Marchelli S, Giuberti T, Fowler P, Chisari FV, Fiaccadori F, Ferrari C. Fine specificity of the human T cell response to hepatitis B virus core antigen. *Arch Virol Suppl* 1992;4:23–28.
 24. Chuang WL, Omata M, Ehata T, Yokosuka O, Ito Y, Imazeki F, Lu SN, Chang WY, Ohto M. Precore mutations and core clustering mutations in chronic hepatitis B virus infection. *Gastroenterology* 1993;104:263–271.
 25. Ehata T, Omata M, Chuang WL, Yokosuka O, Ito Y, Hosoda K, Ohto M. Mutations in core nucleotide sequence of hepatitis B virus correlate with fulminant and severe hepatitis. *J Clin Invest* 1993;91:1206–1213.
 26. Akarca US, Lok AS. Naturally occurring hepatitis B virus core gene mutations. *Hepatology* 1995;22:50–60.
 27. Bozkaya H, Ayola B, Lok AS. High rate of mutations in the hepatitis B core gene during the immune clearance phase of chronic hepatitis B virus infection. *Hepatology* 1996;24:32–37.
 28. Yuan TT, Sahu GK, Whitehead WE, Greenberg R, Shih C. The mechanism of an immature secretion phenotype of a highly frequent naturally occurring missense mutation at codon 97 of human hepatitis B virus core antigen. *J Virol* 1999;73:5731–5740.
 29. Schormann W, Kraft A, Ponsel D, Bruss V. Hepatitis B virus particle formation in the absence of pregenomic RNA and reverse transcriptase. *J Virol* 2006;80:4187–4190.
 30. Heger-Stevic J, Zimmermann P, Lecoq L, Bottcher B, Nassal M. Hepatitis B virus core protein phosphorylation: identification of the SRPK1 target sites and impact of their occupancy on RNA binding and capsid structure. *PLoS Pathog* 2018;14:e1007488.
 31. Wu SY, Chang YS, Chu TH, Shih C. Persistence of hepatitis B virus DNA and the tempos between virion secretion and genome maturation in a mouse model. *J Virol* 2019;93.
 32. Shih C, Wu SY, Chou SF, Yuan TT. Virion secretion of hepatitis B virus naturally occurring core antigen variants. *Cells* 2020;10.
 33. Chua PK, Wang RY, Lin MH, Masuda T, Suk FM, Shih C. Reduced secretion of virions and hepatitis B virus (HBV) surface antigen of a naturally occurring HBV variant correlates with the accumulation of the small S envelope protein in the endoplasmic reticulum and Golgi apparatus. *J Virol* 2005;79:13483–13496.
 34. Yuan TT, Shih C. A frequent, naturally occurring mutation (P130T) of human hepatitis B virus core antigen is compensatory for immature secretion phenotype of another frequent variant (I97L). *J Virol* 2000;74:4929–4932.
 35. Chua PK, Wen YM, Shih C. Coexistence of two distinct secretion mutations (P5T and I97L) in hepatitis B virus core produces a wild-type pattern of secretion. *J Virol* 2003;77:7673–7676.
 36. Ning B, Shih C. Nucleolar localization of human hepatitis B virus capsid protein. *J Virol* 2004;78:13653–13668.
 37. Roseman AM, Berriman JA, Wynne SA, Butler PJ, Crowther RA. A structural model for maturation of the hepatitis B virus core. *Proc Natl Acad Sci U S A* 2005;102:15821–15826.
 38. Bottcher B, Nassal M. Structure of mutant hepatitis B core protein capsids with premature secretion phenotype. *J Mol Biol* 2018;430:4941–4954.
 39. Murayama A, Momose H, Yamada N, Hoshi Y, Muramatsu M, Wakita T, Ishimaru K, Hamaguchi I, Kato T. Evaluation of in vitro screening and diagnostic kits for hepatitis B virus infection. *J Clin Virol* 2019;117:37–42.
 40. Iwamoto M, Watashi K, Tsukuda S, Aly HH, Fukasawa M, Fujimoto A, Suzuki R, Aizaki H, Ito T, Koizumi O, Kusuhara H, Wakita T. Evaluation and identification of hepatitis B virus entry inhibitors using HepG2 cells overexpressing a membrane transporter NTCP. *Biochem Biophys Res Commun* 2014;443:808–813.
 41. Konig A, Yang J, Jo E, Park KHP, Kim H, Than TT, Song X, Qi X, Dai X, Park S, Shum D, Ryu WS, Kim JH,

- Yoon SK, Park JY, Ahn SH, Han KH, Gerlich WH, Windisch MP. Efficient long-term amplification of hepatitis B virus isolates after infection of slow proliferating HepG2-NTCP cells. *J Hepatol* 2019;71:289–300.
42. Otoguro T, Tanaka T, Kasai H, Kobayashi N, Yamashita A, Fukuhara T, Ryo A, Fukai M, Taketomi A, Matsuura Y, Moriishi K. Establishment of a cell culture model permissive for infection by hepatitis B and C viruses. *Hepatol Commun* 2020;5:634–649.
 43. Yamada N, Murayama A, Shiina M, Aly HH, Iwamoto M, Tsukuda S, Watashi K, Tanaka T, Moriishi K, Nishitsuji H, Sugiyama M, Mizokami M, Shimotohno K, Muramatsu M, Murata K, Kato T. Anti-viral effects of interferon-lambda3 on hepatitis B virus infection in cell culture. *Hepatol Res* 2020;50:283–291.
 44. Yamada N, Sugiyama R, Nitta S, Murayama A, Kobayashi M, Okuse C, Suzuki M, Yasuda K, Yotsuyanagi H, Moriya K, Koike K, Wakita T, Kato T. Resistance mutations of hepatitis B virus in entecavir-refractory patients. *Hepatol Commun* 2017;1:110–121.
 45. Sugiyama M, Tanaka Y, Kato T, Orito E, Ito K, Acharya SK, Gish RG, Kramvis A, Shimada T, Izumi N, Kaito M, Miyakawa Y, Mizokami M. Influence of hepatitis B virus genotypes on the intra- and extracellular expression of viral DNA and antigens. *Hepatology* 2006;44:915–924.
 46. Suzuki Y, Maekawa S, Komatsu N, Sato M, Tatsumi A, Miura M, Matsuda S, Muraoka M, Nakakuki N, Shindo H, Amemiya F, Takano S, Fukasawa M, Nakayama Y, Yamaguchi T, Inoue T, Sato T, Sakamoto M, Yamashita A, Moriishi K, Enomoto N. Hepatitis B virus (HBV)-infected patients with low hepatitis B surface antigen and high hepatitis B core-related antigen titers have a high risk of HBV-related hepatocellular carcinoma. *Hepatol Res* 2019;49:51–63.
 47. Seitz S, Iancu C, Volz T, Mier W, Dandri M, Urban S, Bartenschlager R. A slow maturation process renders hepatitis B virus infectious. *Cell Host Microbe* 2016;20:25–35.
 48. Abe A, Inoue K, Tanaka T, Kato J, Kajiyama N, Kawaguchi R, Tanaka S, Yoshida M, Kohara M. Quantitation of hepatitis B virus genomic DNA by real-time detection PCR. *J Clin Microbiol* 1999;37:2899–2903.
 49. Chen RW, Piiparinen H, Seppanen M, Koskela P, Sarna S, Lappalainen M. Real-time PCR for detection and quantitation of hepatitis B virus DNA. *J Med Virol* 2001;65:250–256.
 50. Gunther S, Li BC, Miska S, Kruger DH, Meisel H, Will H. A novel method for efficient amplification of whole hepatitis B virus genomes permits rapid functional analysis and reveals deletion mutants in immunosuppressed patients. *J Virol* 1995;69:5437–5444.
 51. Cai D, Nie H, Yan R, Guo JT, Block TM, Guo H. A southern blot assay for detection of hepatitis B virus covalently closed circular DNA from cell cultures. *Methods Mol Biol* 2013;1030:151–161.
 52. Watashi K, Liang G, Iwamoto M, Marusawa H, Uchida N, Daito T, Kitamura K, Muramatsu M, Ohashi H, Kiyohara T, Suzuki R, Li J, Tong S, Tanaka Y, Murata K, Aizaki H, Wakita T. Interleukin-1 and tumor necrosis factor-alpha trigger restriction of hepatitis B virus infection via a cytidine deaminase activation-induced cytidine deaminase (AID). *J Biol Chem* 2013;288:31715–31727.

Received September 8, 2020. Accepted July 26, 2021.

Correspondence

Address correspondence to: Takanobu Kato, MD, PhD, Toyama 1-23-1, Shinjuku-ku, Tokyo 162-8640, Japan. e-mail: takato@nih.go.jp; fax: +81-3-5285-1161.

Acknowledgments

The authors thank Dr Marc Peter Windisch (Institut Pasteur Korea, Seoul, South Korea) for providing the HepG2-NTCPsec+ cell line and Dr Tawfeek H. Abdelhafez for his technical assistance.

Current address: Hironori Nishitsuji, Department of Virology and Parasitology, Fujita Health University School of Medicine, Toyoake, Aichi 470-1192, Japan.

CRedit Authorship Contributions

Takashi Honda (Conceptualization: Equal; Data curation: Equal; Formal analysis: Supporting; Funding acquisition: Supporting; Investigation: Equal; Methodology: Equal; Project administration: Equal; Writing – original draft: Supporting; Writing – review & editing: Supporting)

Norie Yamada (Investigation: Supporting)
 Asako Murayama (Investigation: Supporting)
 Masaaki Shiina (Investigation: Supporting)
 Hussein Hassan Aly (Investigation: Supporting)
 Asuka Kato (Investigation: Supporting)
 Takanori Ito (Investigation: Supporting)
 Yoji Ishizu (Investigation: Supporting)
 Teiji Kuzuya (Investigation: Supporting)
 Masatoshi Ishigami (Investigation: Supporting)
 Yoshiki Murakami (Investigation: Supporting)
 Tomohisa Tanaka (Methodology: Supporting; Resources: Supporting)
 Koji Moriishi (Methodology: Supporting; Resources: Supporting)
 Hironori Nishitsuji (Methodology: Supporting; Resources: Supporting)
 Kunitada Shimotohno (Methodology: Supporting; Resources: Supporting)
 Tetsuya Ishikawa (Investigation: Supporting)
 Mitsuhiro Fujishiro (Supervision: Supporting)
 Masamichi Muramatsu (Supervision: Supporting)
 Takaji Wakita (Supervision: Supporting)

Takanobu Kato, MD, PhD (Conceptualization: Equal; Data curation: Lead; Formal analysis: Lead; Funding acquisition: Lead; Investigation: Lead; Methodology: Lead; Project administration: Lead; Resources: Lead; Writing – original draft: Lead; Writing – review & editing: Lead)

Conflicts of interest

The authors disclose no conflicts.

Funding

Supported by grants for Research Programs on Hepatitis (JP19fk0310103 and JP19fk0310120 for TK and JP15fk0310001 for YM) from the Japan Agency for Medical Research and Development, AMED and by Grant-in-Aid for Scientific Research (JSPS KAKENHI Grant Number 19K08482 for TK and 20K08382 for TH). TK was also supported by the Taiju Life Social Welfare Foundation. The funders had no role in the study design, data collection or interpretation, or decision to submit the work for publication.